

Synthesis, Characterization and Use of Alumina Doped with TiO₂ and ZrO₂ to Produce Biofuels from Soybean Oil by Thermal Cracking, Transesterification and Hydroesterification

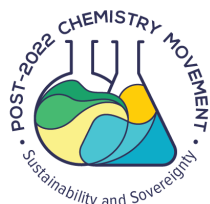
Sarah S. Brum,^a Rafael L. Quirino,^{id b} Leila O. Daher,^a Osvaldo K. Iha,^a
Erick M. Ehlert,^a Joel C. Rubim^a and Paulo A. Z. Suarez^{id *a}

^aLaboratório de Materiais e Combustíveis (LMC), Instituto de Química (IQ),
Universidade de Brasília (UnB), Campus Universitário Darcy Ribeiro, CP 4478,
70919-970 Brasília-DF, Brazil

^bChemistry Department, Georgia Southern University, 30460 Statesboro, GA, USA

In this work, different metal oxides containing Ti, Zr and Al were prepared and characterized and their catalytic activities for cracking, transesterification, and hydroesterification reactions of soybean oil were evaluated. It is described the synthesis of the solids by co-precipitation, and their characterization by thermogravimetry, X-ray diffraction, Brunauer-Emmet-Teller surface area determination, Fourier-transformed Raman spectroscopy, and the determination of Lewis and Brønsted acid sites by pyridine adsorption and detection through Fourier transform infrared spectroscopy (FTIR). The hydrocarbons obtained by soybean pyrolysis were analyzed by fractional distillation, acid number, FTIR, density (at 20 °C), viscosity (at 40 °C), and calculation of the cetane number. The results suggest that all of the solids exhibit catalytic activity at the second stage of the cracking reaction (deoxygenation), lowering the final acidity of the products. The solids also exhibited catalytic activity for transesterification and hydroesterification of triacylglycerides, leading to good yields in methyl fatty acid esters.

Keywords: biofuels, soybean oil, thermal cracking, transesterification, hydroesterification



Introduction

Energy is the basis of all transformation processes. To dominate his environment, human being has constantly searched for a way to control energy in Nature. Right after the Industrial Revolution, and the consequently urbanization of the world, the demand for energy increased considerably. The increasingly use of non-renewable sources of energy gave rise to the uncertainty about how long natural stocks would last. The emission of gases originated from the combustion of fossil fuels triggered concerns about the environment, and the research for cleaner energy sources became very popular in the scientific community.¹ In this context, vegetable, animal or microbial fats and oils have been proposed as interesting renewable starting materials for the production of diesel-like fuels, consisting of a mixture of hydrocarbons and methyl or ethyl fatty acid esters suitable to be used pure or blended with fossil diesel

in regular engines.² The different proposed approaches are illustrated in Figure 1.^{3,4} These processes afford a mixture of compounds with bulk characteristics very similar to those of fossil fuels, but with the advantage of diminishing carbon footprint and are SO_x free.⁵ In this context, the search for robust catalyst that may be used in these different processes is essential to develop biorefineries.

Indeed, a mixture of hydrocarbons can be obtained by the cracking/pyrolysis of triacylglycerides or fatty acids, resulting in oxygenated organic by-products, water, and carbon mono- and di-oxides (Figure 1a). In a different process, methyl or ethyl fatty esters can be produced by different routes, depending on the purity grade of the starting material. For oils or fats with low free fatty acid content, the reaction of choice is the direct transesterification (Figure 1b). However, for high acid fats and oils, combined processes are more suitable, such as the hydrolysis of triacylglycerides (Figure 1c), followed by esterification of fatty acids (Figure 1d). Alternatively, the esterification of free fatty acids with the simultaneous transesterification of triacylglycerides can be employed (Figure 1e).

*e-mail: psuarez@unb.br

Editor handled this article: Luiz Ramos (Guest)

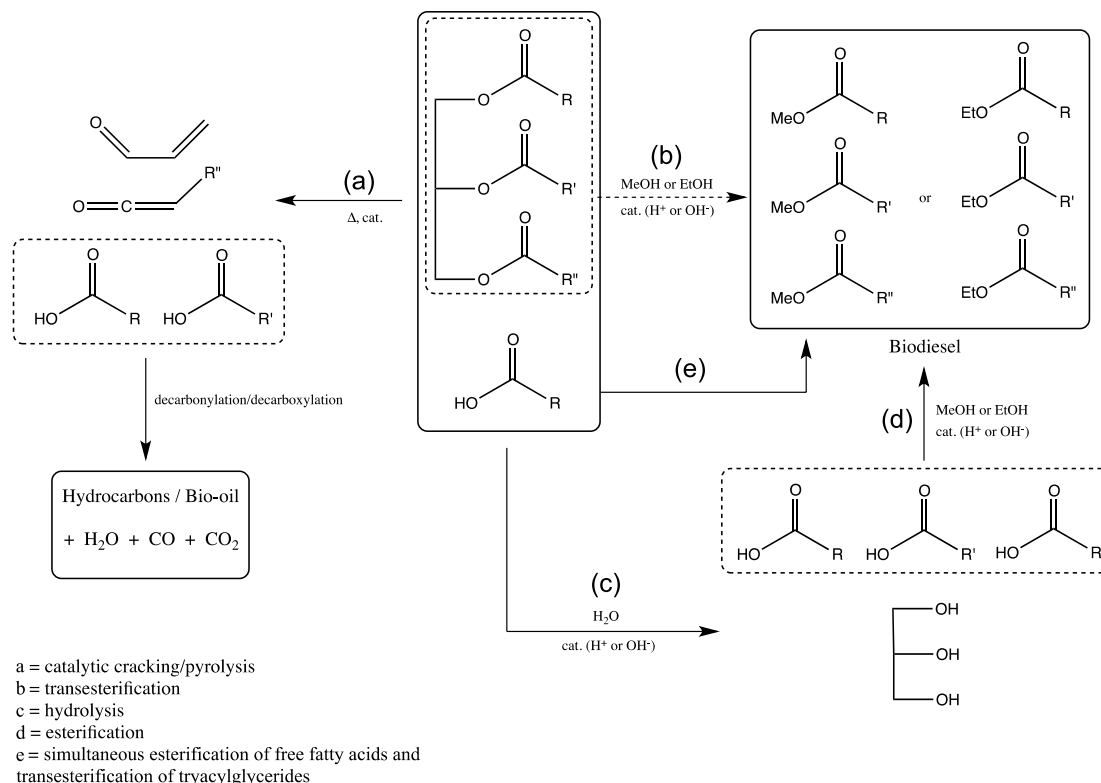


Figure 1. Processing fats and oils to produce biofuels: (a) pyrolysis of triacylglycerides and fatty acids; (b) transesterification of triacylglycerides; (c) hydrolysis of triacylglycerides; (d) esterification of fatty acids; and (e) simultaneous esterification of fatty acids and transesterification of triacylglycerides.

Several catalysts for the transesterification and the cracking of triglycerides have already been developed and tested in an attempt to improve the properties of biofuels produced from those techniques.⁶⁻¹⁰ Most of those catalysts improve the yield of the conversion and reduce the reaction time. Zeolites also reduce the final acidity of pyrolysis products, but they yield hydrocarbons with shorter chains and aromatic compounds.¹¹⁻¹³ The use of certain metal oxides such as MgO and Nb₂O₄ has demonstrated lower yields for the secondary cracking (deoxygenation) and/or the transesterification reaction of vegetable oils.^{6,14}

The triglyceride cracking reaction mechanism, although not completely understood because of its complexity, is partially elucidated in the literature.^{7,10} Different fats and oils have already been tested over the past years as raw materials to produce hydrocarbons, such as usual sources like canola,⁸ and soybean,⁹ or alternative ones like wood,¹⁵ algae,¹⁶ fish¹⁷ and industrial or domestic fatty wastes.^{4,18}

Other recent advances in the catalytic cracking of triglycerides are the search for catalysts and processes that yield biofuels with higher efficiency and/or controlled acidity. Along those lines, sulfated zirconia was successfully employed in the cracking of rapeseed oil.¹⁹ Similarly, HZSM-5 was used to catalyze the conversion of palm oil to gasoline-like bio-fuels.²⁰ The cracking of soybean oil, followed by esterification, results in a less acidic product.²¹

Under controlled cracking conditions, it is possible to favor the formation of cyclic hydrocarbons and aromatics.²²

Various acidic solids, such as sulfated titania,²³ sulfonated polystyrene,²⁴ Amberlyst® resins,²⁵ Nafion,²⁶ heterogeneous heteropolyacids²⁷ and Nb oxides⁶ have also been tested as catalysts for the esterification of fatty acids, and the transesterification of triglycerides. The disadvantages of these acidic solid catalysts are the required elevated temperatures, long reaction time, rapid deactivation, and low conversion yield for materials with high fatty acid content, such as non-refined oils, cooking oil, and fats. Those factors are the consequence of the transesterification by Bronsted acid sites being slower than the esterification reaction, resulting in a final product rich in triglycerides, and requiring a final distillation step in order to isolate the desired products.²⁸⁻³⁰

These problems have been circumvented by the hydrolysis of triglycerides prior to the esterification process, a route known as hydroesterification. It has been demonstrated that the hydroesterification makes use of a variety of starting materials, regardless of fatty acid or moisture content.^{4,31,32} For instance, cadmium oxide³³ and tin ferrite³⁴ have shown excellent activity to produce fatty acid methyl esters using hydroesterification and esterification/transesterification routes of fatty materials regardless their starting purity degree.

In previous works^{9,35} we have developed alumina-based catalysts doped with mild acid metal cations, such as tin and zinc. These catalysts have been shown very active for transesterification of acylglycerols and esterification of fatty acids but not very efficient to promote hydrolysis of esters.³⁵⁻³⁷ We have also shown that these weak acid alumina-based catalysts could promote the deoxygenation of fatty materials pyrolysis' products but in a low rate.⁹ To evaluate the role of catalyst acidity in its activity we decided to prepare doped alumina using more acid metal ions. Thus, searching for robust catalysts that could be used in all reactions shown in Figure 1. Thus, in this work we present the synthesis and characterization of new aluminas doped with zirconium and titanium oxides and study their application for cracking, transesterification, and hydroesterification of soybean oil.

Experimental

Al(NO₃)₃•9H₂O (Sigma-Aldrich, Saint Louis, Missouri, USA), ZrOCl₂•8H₂O (Sigma-Aldrich), TiCl₄ (Sigma-Aldrich), Na₂CO₃•H₂O (Vetec, Duque de Caxias, RJ, Brazil), methanol (Vetec), 2-propanol (Vetec) and hexane (Vetec) were obtained from commercial sources and used as received. Refined soybean oil (Bunge, Valparaíso, GO, Brazil) was purchased from a local grocery store with usual composition (11% palmitic acid, 4% stearic acid, 25% oleic acid, 51% linoleic acid and 9% linolenic acid).

The desired white solids were obtained by the co-precipitation method, based on a previously reported synthesis.³ (TiO₂)₂(Al₂O₃)₄ was prepared by mixing 200 mL of a 0.665 mol L⁻¹ aqueous solution of Al(NO₃)₃•9H₂O, 150 mL of a 0.222 mol L⁻¹ aqueous solution of TiCl₄, and 500 mL of a 1.05 mol L⁻¹ aqueous solution of Na₂CO₃•H₂O and keeping under magnetic during 30 min at room temperature. Then, the mixture was refrigerated at approximately 4 °C for 12 h. The precipitate was filtered, washed three times with distilled water, and dried in an oven kept at 110 °C for 24 h. Then, two different materials were obtained by calcinating at different temperatures (400 and 800 °C). The final solids were then macerated to give particles with diameter inferior than 400 µm. To prepare (ZrO₂)₂(Al₂O₃)₄ solids a similar procedure was performed, using 100 mL of a 0.333 mol L⁻¹ aqueous solution of ZrOCl₂•8H₂O in replacement of the TiCl₄ solution. A similar procedure was performed to prepare (TiO₂)(ZrO₂)(Al₂O₃)₄ solids using 200 mL of a 0.665 mol L⁻¹ aqueous solution of Al(NO₃)₃•9H₂O, 150 mL of a 0.111 mol L⁻¹ aqueous solution of TiCl₄, 100 mL of a 0.167 mol L⁻¹ aqueous solution of ZrOCl₂•8H₂O and 500 mL of a 1.05 M aqueous solution of Na₂CO₃•H₂O.

Pyrolysis reactions

The pyrolysis reactions were performed in a 250 mL three necked round bottom flask with temperatures varying from 350 to 400 °C. In each run, 200 g of soybean oil were heated in the presence of 2 g of catalyst using an electric heating mantle. The temperature of vapors leaving the flask was monitored with thermocouples. Those vapors were condensed in a standard glass condenser and the cracked oil was collected in a graduated cylinder. The reaction was consistently stopped after 150 mL of product was collected. This procedure ensured a consistent comparison of the different solids investigated. Two distinct phases (an aqueous layer and an organic layer) were recovered in the graduated cylinder. The two layers were weighed separately, and the mass of gases was estimated based on the initial mass of soybean oil used and the residue left in the reaction flask.

Transesterification reactions

The transesterification of soybean oil was performed at two distinct temperatures, 70 and 150 °C. At 70 °C, the reaction was performed under reflux conditions, with soybean oil, methanol and the catalyst being kept under magnetic stirring throughout the reaction time. For the reaction performed at 150 °C, a stainless steel reactor equipped with temperature control and magnetic stirrer was used. In either set-up, 20 g of soybean oil was utilized with oil/methanol molar ratios of 4, 6, 9, and 12. Reaction time and catalyst loading were varied as described in the text.

Hydrolysis reactions

The hydrolysis reactions were conducted in a 100 mL Parr 5500 Series Compact Reactor (Moline, IL, United States of America) with temperature control and mechanical stirring. In each reaction, 10.00 g of oil and a 1:50 oil:water molar ratio was used. Because of previous studies³⁵⁻³⁷ carried out using different catalysts on the influence of temperature in the hydrolysis, the reactions were performed at 200 °C and 800 rpm stirring to obtain uniformity in the experiment. 1 wt.% of catalyst (relative to soybean oil weight) was used in each experiment, and three reaction times were evaluated: 2, 4 and 6 h.

Chemical characterization of the solids

Before activation, thermogravimetric analysis (TGA) was carried-out on the synthesized solids in order to determine the best activation temperature. This

experiment was run in a TGA-50 Shimadzu (Tokyo, Japan), with a platinum pan, under air atmosphere and a $20\text{ }^{\circ}\text{C min}^{-1}$ heating rate, with temperatures ranging from room temperature to $800\text{ }^{\circ}\text{C}$. X-ray diffraction experiments were carried out in a Rigaku GeigerFlex diffractometer, model D/MAX-2AC (Tokyo, Japan), operating with a copper tube under 30 kV and 10 mA, with a wavelength of 1.54178 \AA and a scanning rate of $2^{\circ}\text{ min}^{-1}$, with intervals of 0.05° and 2θ varying between 2° and 80° . Raman spectra were obtained in a Bruker Equinox 55 interferometer (Billerica-MA, United States of America) equipped with a Ge detector cooled with liquid nitrogen. A quartz cuvette with retro-scattering geometry and optical path of 1 cm was used to hold the samples. Brunauer-Emmet-Teller (BET) surface area was determined in a Micromeritics analyzer, model ASAP 2010.31 (Norcross-GA, United States of America), with adsorption and desorption isotherms at 77 K. The chemical composition of the solids was established using an induced coupled plasma atomic emission spectrometry (ICP-AES) device. 20 mg samples of each solid were digested in 10 mL of aqua regia during 1.5 h at $100\text{ }^{\circ}\text{C}$. The samples were then diluted to 50 mL with deionized water. Duplicate measurements were obtained in a Varian Liberty RL Series II spectrometer (Palo Alto-CA, United States of America). In order to determine the actual concentration of Ti, Al and Zr in the samples, a previously established calibration curve with 0.5 and 10.0 limits and correlation coefficient superior than 0.9999 was used. The determination of Bronsted (B) and Lewis (L) acid sites in the solids was conducted by pyridine adsorption and Fourier transform infrared (FTIR) detection, following a procedure previously described in the literature.³⁸ The FTIR spectra were obtained through KBr discs containing 0.5 mg of the solid sample. In these experiments, a spectrometer BOMEM-MB series (Quebec, Canada) was used and the final spectra correspond to the average of 10 scans between 400 and 4000 cm^{-1} .

Characterization of the pyrolysis products

The organic layer obtained from the pyrolysis reaction was characterized by acid number (ASTM-D465-9),³⁹ FTIR (Bruker Equinox 55, NaCl window method), density at $20\text{ }^{\circ}\text{C}$ (ASTM-D1298),⁴⁰ viscosity (ASTM-D445),⁴¹ cetane number (ASTM-D613),⁴² gas chromatography mass spectrometry (GC-MS, Shimadzu GCMS-QP5050, Kyoto, Japan), and gas chromatography-flame ionization detection (GC-FID, Shimadzu GC-17A, Kyoto, Japan). The gas chromatographs used were equipped with polydimethylsiloxane columns (length: 50 m, internal diameter: 0.25 mm and layer: 0.2 μm ,

CBPI PONA-M50-042). Chromatography experiments were conducted between 50 and $250\text{ }^{\circ}\text{C}$, with a $10\text{ }^{\circ}\text{C min}^{-1}$ heating rate. Finally, the organic product was distilled following ASTM-D86⁴³ in a HERZOG automatic distiller, model HDA-627 (Osnabrück, Germany), giving the composition of the product by distillation temperature ranges.

Characterization of the transesterification products

Transesterification products were analyzed by high performance liquid chromatography (HPLC) on a Shimadzu CTO-20A apparatus (Kyoto, Japan) equipped with a UV-Vis detector, with detection at 205 nm. A VP-ODS Shim-Pack column (C-18 250 mm 4.6 mm i.d. (Kyoto, Japan)), an injection volume of 10 μL , and a flow rate of 1.0 mL min^{-1} were used in all experiments. The column temperature was maintained at 313 K. All samples were dissolved in a 5:4 v/v mixture of 2-propanol and hexane, and analyzed in a binary linear gradient of 18.5 min running. Initially, 100% methanol was used at 0 min, incremental additions of the 2-propanol/hexane mixture were carried out until a mixture containing 50% of methanol and 50% of 2-propanol/hexane (5:4, v/v) was obtained over 10 min run. An isocratic elution with that same composition followed over the last 8.5 min of the run.

Hydrolysis products

In order to observe the effect of the solids in the hydrolysis reactions, the methodology used to determine fatty acid in oils and fats, described by the American Oil Chemists Society (AOCS method Cd3d63), was followed. Additionally, the same HPLC methodology described for the analysis of the transesterification products was followed.

Results and Discussion

Preparation and characterization of solids

All prepared solids were analyzed by thermogravimetry-derivative thermogravimetry (TG-DTG) and one of the graphs is shown in Figure 2. The TG-DTG analysis of the solids prior to activation revealed three major areas of mass loss. The first one, related to water evolution, was observed at approximately $100\text{ }^{\circ}\text{C}$. The second one, in the $250\text{--}350\text{ }^{\circ}\text{C}$ range, is attributed to the conversion of CO_3^{2-} into CO_2 .⁴⁴ The final major mass loss (at approximately $650\text{ }^{\circ}\text{C}$) relates to the loss of surface acidity in the form of H_2O .⁴⁵ From the TGA results, two activation temperatures were chosen (400 and $800\text{ }^{\circ}\text{C}$) and a total of six different solids were obtained, as shown in Table 1.

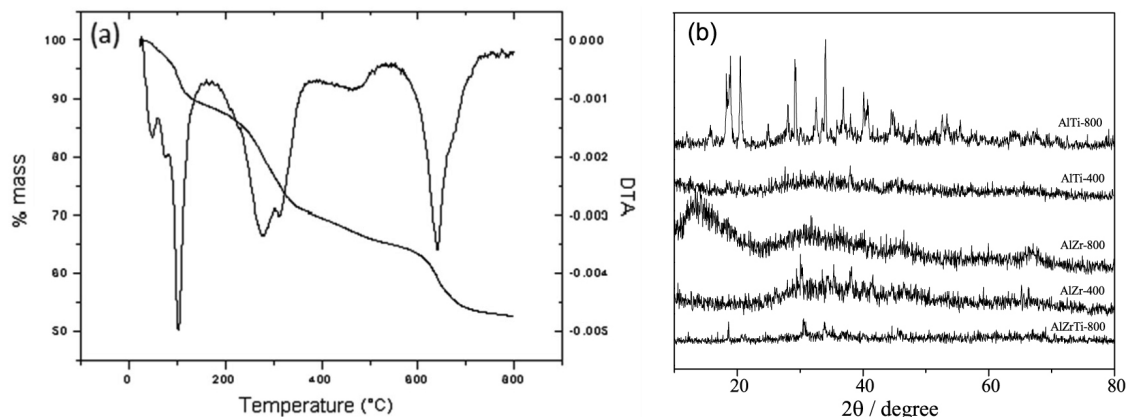


Figure 2. Prepared mixed oxides characterization: (a) TGA and DTG of $(\text{ZrO}_2)_2(\text{Al}_2\text{O}_3)_4$; and (b) X-ray diffractograms of the 5 activated solids.

Table 1. Six mixed oxides prepared solids: chemical composition and texture properties

Sample	Chemical formula	Activation temperature / °C	Surface area / ($\text{m}^2 \text{g}^{-1}$)	Pore diameter / nm	LAS ^a / ($\mu\text{mol mg}^{-1}$)	BAS ^b / (mmol mg^{-1})
Ti/Al-400	$(\text{TiO}_2)_2(\text{Al}_2\text{O}_3)_4$	400	16.263	10.735	83.38	365.43
Ti/Al-800	$(\text{TiO}_2)_2(\text{Al}_2\text{O}_3)_4$	800	4.183	13.092	94.54	333.75
Zr/Al-400	$(\text{ZrO}_2)_2(\text{Al}_2\text{O}_3)_4$	400	6.715	6.709	75.42	205.13
Zr/Al-800	$(\text{ZrO}_2)_2(\text{Al}_2\text{O}_3)_4$	800	3.700	7.791	110.96	101.01
Ti/Zr/Al-400	$(\text{TiO}_2)(\text{ZrO}_2)(\text{Al}_2\text{O}_3)_4$	400	11.622	10.717	106.56	46.03
Ti/Zr/Al-800	$(\text{TiO}_2)(\text{ZrO}_2)(\text{Al}_2\text{O}_3)_4$	800	4.405	11.170	103.24	84.75

^aLewis acid sites; ^bBronsted acid sites.

As can be depicted from Figure 2b, the X-ray diffraction patterns for each activated solid showed a low degree of crystallinity, with some similarities with γ -alumina.⁴⁶ The absence of zirconia and titania peaks suggests that those structures did not form as a segregate phase and these oxides were probably integrated in the alumina network.^{47,48}

A comparison of the FT-Raman spectra of the solids activated at 400 and 800 °C, as can be depicted from

Figure 3, reveal the disappearance of the carbonate peaks at 180, 730, 1067, and 1387 cm^{-1} for the solids activated at the higher temperature.⁴⁹ Also, the intensity of the peak at 1079 cm^{-1} is much lower for the solids activated at 800 °C, indicating partial carbonate degradation upon heating. Nonetheless, the presence of that peak suggests that carbonate is still present in the solids' network, most likely contributing to the formation of amorphous regions in the solids' structure.

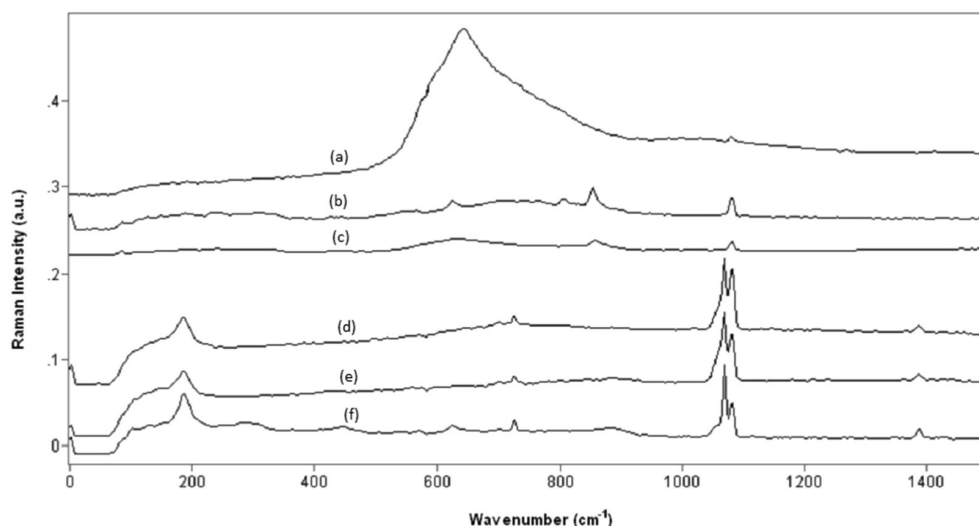


Figure 3. FT-Raman spectra of the 6 activated solids: (a) Zr/Al-800; (b) Ti/Zr/Al-800; (c) Ti/Al-800; (d) Zr/Al-400; (e) Ti/Zr/Al-400; and (f) Ti/Al-400.

The chemical composition, as determined by ICP-AES analysis, confirmed the expected molecular formulas of the solids. A summary of those results can be found in Table 1. It can be concluded that Zr atoms did not insert in the solids' network as well as Ti atoms. This fact could be related to Zr's bigger atomic radius.

The BET surface area and pore size of the solids studied are summarized in Table 1. All solids presented isotherms of the type IV, indicating the presence of mesoporous. This is corroborated by Barrett-Joyner-Halenda (BJH) method, that showed porous diameters in the range of 50 to 200 Å. Although small surface areas were obtained for the solids, interesting information can be extracted from the analysis of the results in Table 1. For example, the solids containing Zr presented the lowest values for surface area and pore size.

Table 1 also shows the results obtained for the distribution of Lewis and Bronsted acid sites in the solids' surface. These results suggest that the activation temperature influences the surface acidity of the solids. The solids activated at 400 °C exhibit more Bronsted acid sites (B) than those activated at 800 °C. This fact is most likely due to the dehydroxylation mentioned earlier by Kovanda *et al.*⁴⁵ Also, there is no significant variation on the number of Lewis acid sites (L) for different solids treated at the same temperature. This indicates that (L) sites are probably related to the presence of Al atoms, and independent from Ti and Zr. The increase in Lewis acid sites for samples activated at 800 °C relates to a greater exposition of internal sites due to larger pores.

Hydrocarbons production by soybean oil cracking in the presence of the prepared solids

Table 2 summarizes the primary results obtained after the pyrolysis reaction of soybean oil in the presence of

the synthesized solids. In order to ensure consistency, the numbers presented in Table 2 correspond to the average of duplicate experiments.

A good correlation between the yield in cracking products and the amount of residue left in the reaction flask can be seen. For example, the reaction with the highest yield (thermal) also presents the lowest amount of residue. The inverse is observed for Zr/Al-800 (1.0 g). When considering the formation of water, it can be consistently seen that all experiments conducted in the presence of the solids resulted in a higher yield of water than the thermal experiment. This is an evidence that corroborates the idea of a decarbonylation path for the degradation of carboxylic acids.¹⁰ The highest yield in water was observed in the presence of Ti/Al-400, and the lowest yield of water was observed in the presence of Ti/Al-800. Thus, it is reasonable to conclude that the highest acidity the higher decarbonylation yield. Note that lower decarbonylation rates were achieved in a previous work⁷ using less acid alumina and zinc and tin mixed oxides under similar conditions, which corroborate the result observed here. Furthermore, different amounts of a solid showed an influence in the final content of water, indicating that a higher contact surface favors the degradation of carboxylic groups.

A correlation can be observed between the amount of water formation, the acid number (AN) and the integration of the peak at 1715 cm⁻¹ (carbonyl of carboxylic acids) in the FTIR spectrum of the products (Table 2). The spectra were normalized with respect to the peak at 2850 cm⁻¹ (bending of the C(sp³)-H bond) and the values for integration were assigned taking the lowest area as being 0.00 and the highest as 1.00, the other values were distributed relative to these two marks.

According to Table 2, the highest amount of water

Table 2. Soybean oil pyrolysis assisted by the synthesized solids: mass balance and characterization of the organic phase (acid number (AN), relative integration of (C=O) peak and hydrocarbons/oxygenated compounds percentage)^a

Solid	Organic layer / g	Water / g	Vapor / g	Residue / g	AN / (mg KOH g ⁻¹ of product)	Relative integration (C=O)	Hydrocarbon / %	Oxygenated compounds / %
Ti/Al-400	65.5	3.5	8.0	23.0	75.53	0.00	79.9	20.1
Ti/Al-800	61.0	2.0	13.0	24.0	88.04	0.25	69.7	30.3
Zr/Al-400	61.5	3.0	8.5	27.0	85.94	0.08	70.9	29.1
Zr/Al-800 (0.5 g)	68.5	2.0	10.0	19.5	ND ^b	ND ^b	63.8	36.2
Zr/Al-800 (1.0 g)	59.0	2.5	13.5	25.0	92.07	0.21	64.1	35.9
Zr/Al-800 (1.5 g)	65.0	3.0	10.5	21.5	ND ^b	ND ^b	69.4	30.6
Ti/Zr/Al-400	60.0	3.0	11.0	26.0	83.84	0.06	65.5	34.4
Ti/Zr/Al-800	63.5	2.5	13.0	21.0	84.98	0.10	68.6	31.4
Thermal ^c	70.0	1.0	12.0	17.0	112.64	1.00	62.7	37.7

^aReaction temperatures varied in the range of 350 to 400 °C; ^bND: not determined; ^cthe reaction was carried-out in the absence of solids.

formed corresponds to the lowest acid number and the lowest FTIR integration (Ti/Al-400). In the thermal experiment, it was observed the lowest amount of water formation and the highest values for IR integration and acid number. Even though the reactivity of all solids is very similar, it is evident that all of them showed a significant reduction in the final acidity of the pyrolysis products.

The data obtained from the GC analyses were summarized into percentage of oxygenated and non-oxygenated products and are also presented in Table 2. Although very similar, the results presented in Table 2 confirm the higher activity of Ti/Al-400 when compared to the other solids. Indeed, reactions in the presence of this solid exhibit the highest percentage of non-oxygenated products (79.9%), while the thermal experiment exhibits the lowest value with 62.7% of non-oxygenated products.

Table 3 shows the main physical-chemical properties of the cracking organic products obtained in the reactions presented in Table 2. As can be depicted, the use of all of the solids resulted in density values in agreement with Brazilian regulation (ANP No. 50 December, 23rd 2013)⁵⁰ for diesel fuel (ranging from 861 to 872 kg m⁻³). For the viscosity, the sample obtained using the solid Zr/Al-800-1.0 g (6.0 cSt) fell outside the specified range for diesel, while the use of all of the other solids yielded values in agreement with the regulated range. The same trend is observed for the cetane number, all values agreed with the specified range, except for Zr/Al-800 (38) whose value fell below the minimum accepted value (42). All the numbers obtained for the thermal experiment were close to but outside the allowed ranges.

Table 3 also shows the distribution of the products' distilled fractions by temperature ranges. From the similarity of the distribution independently of the solid used, it can be assumed that the solids were similarly active for reactions involving cleavage of C-C bonds, aromatizations or cyclizations. Indeed, a maximum

difference of 5% was observed for the yield in the fraction distilling over 200 °C (Ti/Al-400 and Zr/Al-800, 0.5 g).

Methyl-esters production by soybean oil transesterification in the presence of the prepared solids

The solids listed in Table 1 have also been evaluated in the transesterification of soybean oil with methanol. Initially, the reaction was performed at 70 °C, with various soybean oil/methanol molar ratios (MR). Qualitatively, the products obtained using Ti/Al-400 and Zr/Al-400 were easily separated by centrifugation. The yields obtained for reactions with Ti/Al-800 and Zr/Al-800 are shown in Figure 4a. Similar trends were obtained regardless of the solid used in the reaction. It is noted that increasing the molar ratio from 4 to 6 led to a significant increase in the reaction yield from ca. 50 to ca. 79% for Ti/Al-800, and from ca. 40 to ca. 82% for Zr/Al-800. Further increase of the molar ratio to 9 did not result in a significant change of the reaction yield.

In order to optimize the reaction parameters, the molar ratio was set at 6 and the catalyst loading was modified to 2.5 wt.%, with reaction times varying from 0.5 to 8 h (Figure 4c). It is observed that yields of 70 and 60% were obtained after 4 h for Ti/Al-800 and Zr/Al-800, respectively. These yields have not significantly changed between 4 and 8 h.

The reaction yield can also be maximized by increasing the reaction temperature and/or the soybean oil:methanol molar ratio. The yields of reactions carried out at 150 °C are presented in Figure 5a. An overall increase in the reaction yield with MR can be seen. An optimum yield of 93% was obtained using MR = 12 and Ti/Zr/Al-800.

The reaction yields for experiments carried out in the presence of 2.5 or 1 wt.% of Ti/Al-400, or Zr/Al-400 are presented in Figure 5a. It was observed that catalyst

Table 3. Physical properties of the hydrocarbon mixture obtained by soybean oil pyrolysis products

Solid	Cetane number	Density (20 °C) / (kg m ⁻³)	Viscosity / cSt	Distillation temperature fraction / mass%			
				< 80 °C	80-140 °C	140-200 °C	> 200 °C
Ti/Al-400	41	861	3.9	3	6	10	81
Ti/Al-800	41	867	4.7	2	6	8	84
Zr/Al-400	41	867	4.7	2	6	8	84
Zr/Al-800 (0.5 g)	36	877	6.5	3	4	6	87
Zr/Al-800 (1.0 g)	38	872	6.0	2	5	7	86
Zr/Al-800 (1.5 g)	38	873	9.0	2	5	7	86
Ti/Zr/Al-400	41	862	4.1	2	7	9	82
Ti/Zr/Al-800	40	869	4.8	2	6	8	84
Thermal	37	885	5.7	1	6	7	86
Brazilian regulation	42 (min)	820-880	2.5-5.5	-	-	-	-

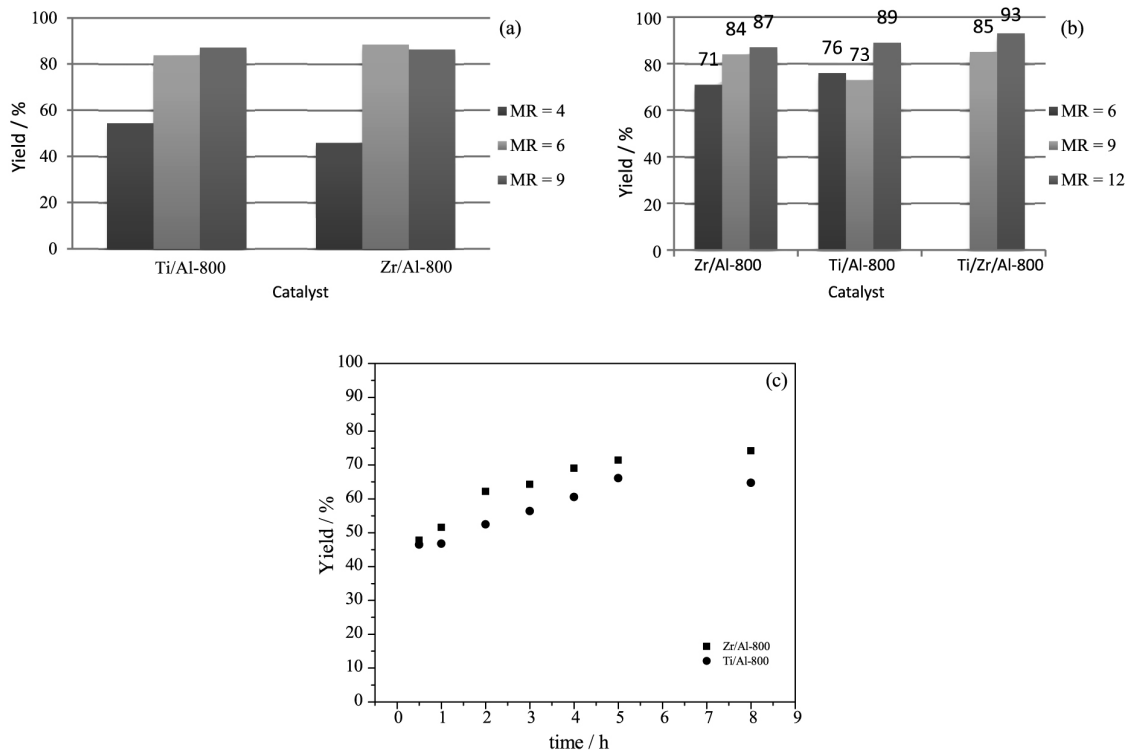


Figure 4. Reaction yields for transesterification of soybean oil with methanol carried out under different conditions: (a) in the presence of 5 wt.% of Ti/Al-800 or Zr/Al-800 at 70 °C in 4 h, using soybean oil:methanol molar ratio (MR) = 4, 6, and 9; (b) in the presence of 2.5 wt.% of Ti/Al-800, Zr/Al-800, or Ti/Zr/Al-800 at 150 °C for 4 h, using MR = 6, 9 and 12; (c) kinetic study of soybean oil transesterification using 2.5 wt.% Ti/Al-800 or Zr/Al-800 with MR = 6.

loading has a very little effect in the yield of methyl esters formation. The reaction performed with 1 wt.% of catalyst and 4 h of reaction time exhibit similar yields, regardless of the solid used. When the reaction time was reduced to 2 h, yields > 80% were observed.

A kinetic study was carried out in order to verify the best reaction parameters for a catalyst loading of 1 wt.% (Figure 5b). It is observed that for either solid, a maximum yield of approximately 85% was obtained. When the reaction is performed in the presence of Ti/Al-400, the maximum yield is attained after 1 h, followed by a decrease to 74% after 2 h, and returning to approximately 80% after 3 h. For Zr/Al-400, the highest yield was achieved after 2 h,

with a slow decrease in yield after that. A comparison of the results of the transesterification of soybean oil in the presence of solids activated at 800 and 400 °C reveals no significant difference in the obtained yields.

Methyl-esters production by soybean oil hydroesterification in the presence of the prepared solids

During transesterification experiments, it was observed that the catalyst activation temperature did not significantly affect the reaction yields. Therefore, it has been decided that only solids activated at 400 °C would be evaluated for hydrolysis reactions. Two standards were used as

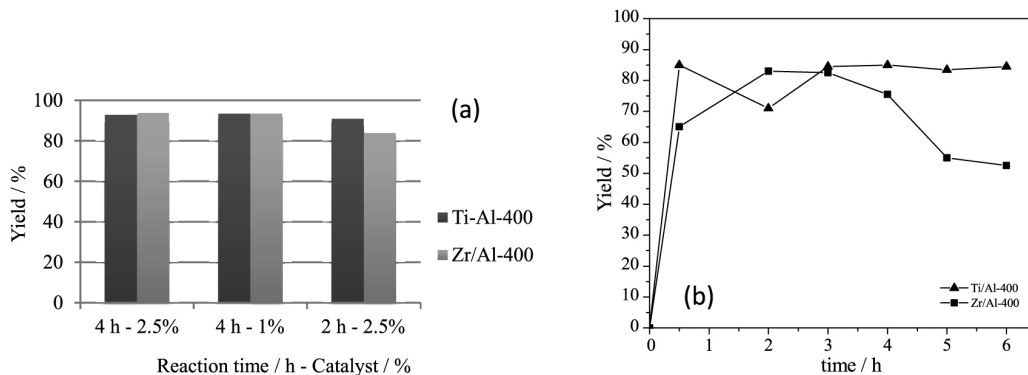


Figure 5. Transesterification of soybean oil with methanol using Ti/Al-400 or Zr/Al-400: (a) using 1 or 2.5 wt.% of the solid at 150 °C and MR = 12; (b) kinetic study.

reference for beginning and end of the hydrolysis. The beginning standard was defined as the product of a reaction involving soybean oil and water (1:50 molar ratio, soybean oil:water) heated at 200 °C and agitated at 800 rpm for 4 h, without any solid. This standard exhibited an acid index of 29.01 mg_(KOH) per g_(sample). For the final standard, the product from the saponification of soybean oil followed by acidification was used. The protocol followed is known to result in 100% conversion of triglycerides into free fatty acids.²⁸ The standard produced exhibited an acid index of 194.0 mg_(KOH) per g_(sample). With the establishment of these two reference numbers, it was possible to compare the catalytic effects of the different solids investigated for the hydrolysis of soybean oil. These results are summarized in Table 4. A comparison of the results from Table 4 with those obtained for the initial standard reveals that after 4 h, all solids showed a considerable increase (> three-fold) in acid index. The results in Table 4 also indicate that Ti/Al-400 and Zr/Al-400 are active for the hydrolysis of soybean oil independent of the catalyst loading used.

Table 4. Relative acid index for the hydrolysis of soybean oil after 4 h in the presence of varying loadings of Ti/Al-400 and Zr/Al-400

Solid	Catalyst loading / wt. %	Acid index / %
Ti/Al-400	1.0	71
Ti/Al-400	2.5	82
Ti/Al-400	5.0	72
Zr/Al-400	1.0	80
Zr/Al-400	2.5	80
Zr/Al-400	5.0	79

A better picture of the reaction kinetics can be obtained by comparing the relative acid index of the products as a function of reaction time (Figure 6). Close analysis of the results presented in Figure 6 helps one to

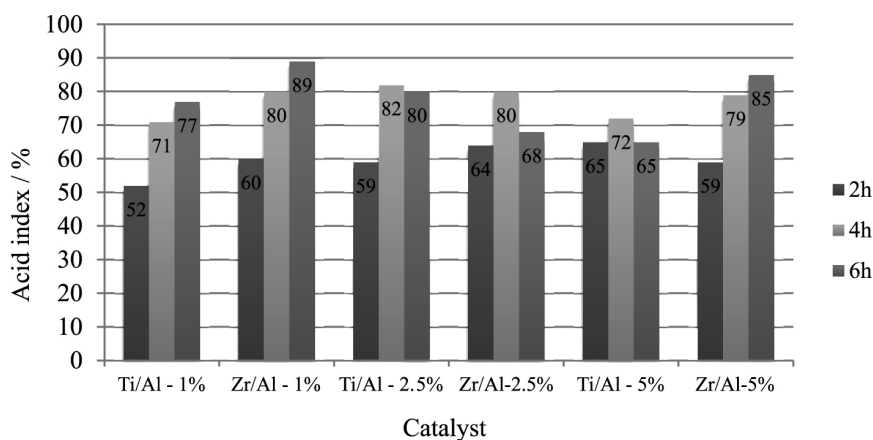


Figure 6. Hydroesterification of soybean oil: relative acid index for the hydrolysis of soybean oil in the presence of Ti/Al-400 and Zr/Al-400 as a function of time and catalyst loading.

identify the optimum reaction conditions (i.e., catalyst loading and reaction time) for the hydrolysis of soybean oil, and establish its equilibrium point. According to the results obtained, free fatty acid yield is maximized when the reaction is carried-out in the presence of 1 wt.% of Zr/Al-400 for 6 h. In this case the relative acid index obtained corresponds to 89% (Figure 6). It is also noticed that very similar results and trends are obtained when 5 wt.% of Zr/Al-400 is employed in the hydrolysis of soybean oil.

With the objective of shifting the equilibrium of the reaction and maximize the yield in free fatty acids,⁵¹ the hydrolysis was performed in two steps. After removing glycerin and water from the reaction mixture, distilled water was added to the product. A displacement of the equilibrium was observed in direction of the desired products. When comparing the 4 h reaction (80% free fatty acid (FFA)) with the reaction in two steps, it is observed that there is an increase in yields for the latter. This increase can be seen in the reaction carried-out in two steps of 2 h (Table 5). The reaction that exhibits the best result is the reaction involving two steps of 4 h. This reaction presented a yield of 98%. Specific reaction times and the results are described in Table 5.

Table 5. Reaction times and corresponding relative acid index soybean oil hydrolysis products in the presence of 1.0 wt.% of Zr/Al-400

Step 1	Reaction time / h		Yield / %
	Step 1	Step 2	
2	2	2	87
4	2	2	88
4	4	4	98

These results indicate that the hydrolysis carried out in two steps is an interesting alternative for the preparation of free fatty acids from triglycerides. These findings can

be demonstrated by HPLC analysis. The triglyceride peaks (12.5–20 min) and the diglyceride peaks (7.6–12.5 min) almost disappear after the reaction, leaving only peaks related to FFAs (2.5–5.8 min), indicating that the reaction in two steps shifts the reaction equilibrium towards product formation, while the catalyst still exhibits activity during the process.

Thus, pure soybean fatty acids were esterified with methanol in the presence of different solids. Different as observed for transesterification and hydrolysis, the solids containing zirconium in their composition presented higher yields than when only titanium were mixed with aluminum. In the presence of Zr/Al it was also observed a strong influence of temperature in the reaction yield, varying from 30% at 120 °C to 80% at 150 °C.

Finally, the catalyst Zr/Al-400 was recovered from reaction and recycled using a new load of soybean oil. The first cycle resulted in an acid value of 109 mg_(KOH) per g_(sample). The second cycle resulted in an acid index of 43 mg_(KOH) per g_(sample), and the third cycle resulted in an acid index of only 5.3 mg_(KOH) per g_(sample). The dramatic decrease in the observed yield may have been caused by several factors, such as loss of catalyst activity by poisoning of the active sites with reaction impurities, or loss of catalyst during the reaction by leaching. In order to verify these two hypotheses, two qualitative ICP experiments were carried-out. In the first experiment, a comparison of the catalyst after and before hydrolysis was performed. On the second experiment, analysis of the organic products (FFA) for detection of zirconium was performed. The result of catalyst analysis by ICP before the reaction indicated the presence of 119 ppm of Zr in the solid used. After the reaction, the resulting value was 124 ppm. These numbers show that there has probably not been Zr leaching from the catalyst during the reaction. In the second analysis, 1.71 ppm of Zr was detected in the FFAs, which is close to the error associated to the instrument used. With these results, it is possible to affirm that it is more likely to have occurred poisoning of the catalyst than leaching.

Conclusions

In this paper it was presented the synthesis and characterization of 6 mixed oxides of the type (TiO₂)_x(ZrO₂)_y(Al₂O₃)_z and their catalytic activities for the pyrolysis, transesterification and hydroesterification of soybean oil were evaluated. It was determined that all the solids were active for the deoxygenation of fatty materials (presumably by the decarbonylation route). The physical properties of the hydrocarbon mixture obtained were in agreement with Brazilian specification for diesel fuel for

almost all the samples obtained. The catalysts were also active to produce fatty acids methyl esters from soybean oil by transesterification and hydroesterification.

Doping alumina with titanium and zirconium oxide higher acidity of the materials were found when compared with those previously described using alumina doped with zinc and tin oxides. These higher acidities improved the performance of all the materials in promoting the deoxygenation of soybean oil under similar conditions. On the other hand, these higher acidity did not compromised the performance of these new solids in promoting transesterification and hydroesterification, leading to similar reaction yields as observed for the weaker acidity materials studied before.

Acknowledgments

The authors are thankful to CNPq, FAP-DF and CAPES for financial support. P. A. Z. S. also wishes to thank CNPq for research fellowship.

Author Contributions

Sarah S. Brum was responsible for the formal analysis, investigation, methodology, writing original draft, writing review and editing; Rafael L. Quirino for the formal analysis, investigation, methodology, writing original draft; Leila O. Daher for the formal analysis and investigation; Osvaldo K. Iha for the formal analysis and investigation; Erick M. Ehlert for the formal analysis and investigation; Joel C. Rubim for the conceptualization, funding acquisition, investigation; Paulo A. Z. Suarez for the conceptualization, funding acquisition, investigation, project administration, writing original draft, writing review and editing.

References

1. Liu, R.; Sarker, M.; Rahmana, M.; Li, C.; Meiyun, C.; Nishu, N.; Cotillon, R.; Scott, N.; *Prog. Energy Combust. Sci.* **2020**, *80*, 100852.
2. Suota, M. J.; Simionatto, E. L.; Scharf, D. L.; Meier, H. F.; Wiggers, V. R.; *Energy Fuels* **2019**, *33*, 9886.
3. Macedo, C. C. S.; Abreu, F. R.; Tavares, A. P.; Alves, M. B.; Zara, L. F.; Rubim, J. C.; Suarez, P. A. Z.; *J. Braz. Chem. Soc.* **2006**, *17*, 1291.
4. dos Santos, L. K.; Hatanaka, R. R.; de Oliveira, J. E.; Flumignan, D. L.; *Renewable Energy* **2017**, *114*, 574.
5. Crabbe, E.; Nolasco-Hipolito, C.; Kobayashi, G.; Sonomoto, K.; Ishizaki, A.; *Process Biochem.* **2001**, *37*, 65.
6. Brandão, R. F.; Quirino, R. L.; Mello, V. M.; Tavares, A. P.; Peres, A. C.; Guinhos, F.; Rubim, J. C.; Suarez, P. A. Z.; *J. Braz. Chem. Soc.* **2009**, *20*, 954.

7. Gusmão, J.; Brodzki, D.; Djéga-Mariadassou, C.; Frety, R.; *Catal. Today* **1989**, *5*, 533.
8. Idem, R. O.; Katikaneni, S. P. R.; Bakhshi, N. N.; *Fuel Process. Technol.* **1997**, *51*, 101.
9. Quirino, R. L.; Tavares, A. P.; Peres, A. C.; Rubim, J. C.; Suarez, P. A. Z.; *J. Am. Oil Chem. Soc.* **2009**, *86*, 167.
10. Vonghia, E.; Boocock, D.; Konar, S.; Leung, A.; *Energy Fuels* **1995**, *9*, 1090.
11. Ooi, Y.; Zakaria, R.; Mohamed, A.; Bhatia, S.; *Energy Fuels* **2005**, *19*, 736.
12. Santos, F. R.; Ferreira, J. C. N.; da Costa, S. R. R.; *Quim. Nova* **1998**, *21*, 560.
13. Sharma, R.; Bakhshi, N.; *Can. J. Chem. Eng.* **1991**, *69*, 1071.
14. Reguera, F.; Araujo, L.; Picardo, M.; Bello, F.; Scofield, C.; Pastura, N.; Gonzalez, W.; *Mater. Res.* **2004**, *7*, 343.
15. Junming, X.; Jianchun, J.; Jie, C.; Yunjuan, S.; *Bioresour. Technol.* **2010**, *101*, 5586.
16. Kwon, E.; Jeon, Y.; Yi, H.; *Bioresour. Technol.* **2012**, *123*, 673.
17. Mrad, N.; Paraschiv, M.; Aloui, F.; Varuvel, E.; Tazerout, M.; Nasrallah, S.; *Int. J. Energy Res.* **2013**, *37*, 1036.
18. Bezergianni, S.; Voutetakis, S.; Kalogianni, A.; *Ind. Eng. Chem. Res.* **2009**, *48*, 8402.
19. Eterigho, E.; Lee, J.; Harvey, A.; *Bioresour. Technol.* **2011**, *102*, 6313.
20. Roesyadi, A.; Hariprajitno, D.; Nurjannah, N.; Savitri, S.; *Bull. Chem. React. Eng. Catal.* **2013**, *7*, 185.
21. Xu, J.; Jiang, J.; Zhang, T.; Dai, W.; *Energy Fuels* **2013**, *27*, 255.
22. Kubatova, A.; St' avova, J.; Seames, W. S.; Luo, Y.; Sadrameli, S. M.; Linnen, M. J.; Baglayeva, G. V.; Smoliakova, I. P.; Kozliak, E. I.; *Energy Fuels* **2012**, *26*, 672.
23. Roperro-Vega, J. L.; Aldana-Pérez, A.; Gómez, R.; Niño-Gómez, M. E.; *Appl. Catal., A* **2010**, *379*, 24.
24. Grossi, C. V.; Jardim, E. O.; Araujo, M. H.; Lago, R. M.; Silva, M. J.; *Fuel* **2010**, *89*, 257.
25. Lopez, D. E.; Goodein Jr., J. G.; Bruce, D. A.; Lotero, E.; *Appl. Catal., A* **2005**, *295*, 97.
26. Ni, J.; Meunier, F. C.; *Appl. Catal., A* **2007**, *333*, 122.
27. Caetano, C. S.; Fonseca, I. M.; Ramos, A. M.; Vital, J.; *Catal. Commun.* **2008**, *9*, 1996.
28. Bala, D. D.; Misra, M.; Chidambaram, D.; *J. Cleaner Prod.* **2017**, *142*, 4169.
29. Singh, S.; Patel, A.; *Ind. Eng. Chem. Res.* **2014**, *53*, 14592.
30. Wang, S.; Xue, Y.; Zhao, X.; Yuan, H.; *Diamond Relat. Mater.* **2021**, *116*, 108420.
31. Suarez, P. A. Z.; Santos, A. L. F.; Rodrigues, J. P.; Alves, M. B.; *Quim. Nova* **2009**, *32*, 768.
32. Sousa, J. S.; Cavalcanti-Oliveira, E. D.; Aranda, D. A. G.; Freire, D. M. G.; *J. Mol. Catal. B: Enzym.* **2010**, *65*, 133.
33. Alves, M. B.; Medeiros, F. C. M.; Suarez, P. A. Z.; *Ind. Eng. Chem. Res.* **2010**, *49*, 7176.
34. Alves, M. B.; Medeiros, F. C. M.; Sousa, M. H.; Rubim, J. C.; Suarez, P. A. Z.; *J. Braz. Chem. Soc.* **2014**, *25*, 2304.
35. Suarez, P. A. Z.; Silva, F. M.; *J. Braz. Chem. Soc.* **2012**, *23*, 1201.
36. Mello, V. M.; Pousa, G. P. A. G.; Pereira, M. S. C.; Dias, I. M.; Suarez, P. A. Z.; *Fuel Process. Technol.* **2011**, *92*, 53.
37. Mello, V. M.; Oliveira, F. C. C.; Fraga, W. G.; do Nascimento, C. J.; Suarez, P. A. Z.; *Magn. Reson. Chem.* **2008**, *46*, 1051.
38. Emeis, C.; *J. Catal.* **1993**, *141*, 347.
39. ASTM D465: *Standard Test Methods for Acid Number of Pine Chemical Products Including Tall Oil and Other Related Products*, West Conshohocken, PA, 2015.
40. ASTM D1298-12b: *Standard Test Method for Density, Relative Density, or API Gravity of Crude Petroleum and Liquid Petroleum Products by Hydrometer Method*, West Conshohocken, PA, 2017.
41. ASTM D445-06: *Standard Test Method for Kinematic Viscosity of Transparent and Opaque Liquids (and Calculation of Dynamic Viscosity)*, West Conshohocken, PA, 2012.
42. ASTM D613-01: *Standard Test Method for Cetane Number of Diesel Fuel Oil*, West Conshohocken, PA, 2017.
43. ASTM D86-12: *Standard Test Method for Distillation of Petroleum Products at Atmospheric Pressure*, West Conshohocken, PA, 2015.
44. Wu, W.; Jiang, Q.; *Mater. Lett.* **2006**, *60*, 2791.
45. Kovanda, F.; Grygar, T.; Dornicak, V.; Rojka, T.; Bezdicka, P.; Jiráková, K.; *Appl. Clay Sci.* **2005**, *28*, 121.
46. Xie, W.; Peng, H.; Chen, L.; *Appl. Catal., A* **2006**, *300*, 67.
47. Kitiyanan, A.; Sakulkhaemareuthai, S.; Suzuki, Y.; Yoshikawa, S.; *Compos. Sci. Technol.* **2006**, *66*, 1259.
48. Li, W.; Li, S.; Zhang, M.; Tao, K.; *Colloids Surf., A* **2006**, *272*, 189.
49. Ali, A. B.; Awaleh, M. O.; Leblanc, L. S. S.; Maisonneuve, V.; Houlbert, S.; *Chimie* **2004**, *7*, 661.
50. Agência Nacional do Petróleo, Gás Natural e Biocombustíveis (ANP); Resolução ANP No. 50, de 23/12/2013; Diário Oficial da União (DOU), Brasília, Brazil, 2013, available at <https://atosoficiais.com.br/anp/resolucao-n-50-2013-atualiza-os-regulamentos-da-anp-em-alinhamento-a-nova-regra-do-controle-da-qualidade-dos-produtos-importados#:~:text=RESOLU%C3%87%C3%83O%20ANP%20N%C2%BA%2050%2C%20DE,24%20DE%20DEZEMBRO%20DE%202013&text=%C2%A7%201%C2%BA%20A%20comercializa%C3%A7%C3%A3o%20de,de%20autoriza%C3%A7%C3%A3o%20pr%C3%A9via%20da%20ANP>, accessed in January 2022.
51. Ma, F.; Hanna, M. A.; *Bioresour. Technol.* **1999**, *70*, 1.

Submitted: September 29, 2021

Published online: January 27, 2022

